Title
Deposition of Monodisperse Particles in Hollow Models Representing Adult and Child-Size Tracheobronchial Airways

Journal
Health Physics, 72(6)

ISSN
0017-9078

Authors
Oldham, MJ
Mannix, RC
Phalen, RF

Publication Date
1997-06-01

DOI
10.1097/00004032-199706000-00001

DEPOSITION OF MONODISPERSE PARTICLES IN HOLLOW MODELS REPRESENTING ADULT AND CHILD-SIZE TRACHEOBRONCHIAL AIRWAYS

Michael J. Oldham, Richard C. Mannix, and Robert F. Phalen*

Abstract—**A series of experiments was performed to determine deposition efficiencies of four sizes of radiolabeled monodisperse particles in custom-made hollow tracheobronchial models. The particles had geometric diameters of about 1, 5, 10, and 15 μm. The tracheobronchial models, consisting of a trachea and two or more additional generations, had dimensions representative of a typical adult, a 7-y-old child, and a 4-y-old child; the child-size models were appropriately scaled-down replicas of the adult-size model. Each deposition experiment was conducted using a steady inspiratory airflow representative of low physical activity for the appropriate age of individual: 20 L min^{-1} for the adult; 9 L min^{-1} for the 7-y-old; 5.5 L min^{-1} for the 4-y-old. The results indicate that deposition efficiency of the particles increased substantially (up to 35 times) in all three models as particle diameter increased from 1–15 μm, undoubtedly as a result of particle impaction and sedimentation-related phenomena. An analysis of variance demonstrated the occurrence of statistically-significant ($p <$ 0.05) main effects of hollow model size and particle size; the interaction between the two parameters was also significant. In general, deposition efficiencies of the various sizes of particles were greater in the child-size models than in the adult-size model; this effect may have risk assessment implications. In addition, the results obtained experimentally agreed more closely with those predicted using a radiation-protection mathematical particle deposition formulation as the particle size increased for each of the sizes of models.**
Health Phys. 72(6):827–834; 1997

Key words: inhalation; aerosols; lungs, human; modeling, dose assessment

INTRODUCTION

A CONSIDERABLE body of work has been published concerning the deposition efficiencies of inhaled particles in the human respiratory tract. Estimates of deposition efficiencies are important for assessment of risks related to exposure to aerosol contaminants. Such estimates have principally used one of two approaches—mathematical modeling or particle deposition experiments. Mathematical modeling-generated predictions of particle deposition generally include three deposition mechanisms (impaction, sedimentation, and diffusion), respiratory tract geometrical parameters, and airflow data (Morrow et al. 1966; Yeh et al. 1976, 1996; Yeh and Schum 1980; Xu and Yu 1986; Phalen et al. 1988; Thomas 1988; Swift 1989; Balásházy et al. 1991; Schum et al. 1994). Recently, the International Commission on Radiological Protection (ICRP) has revised its respiratory tract dosimetry model, and the National Council on Radiation Protection and Measurements (NCRP) has proposed a revision to its respiratory tract dosimetry model (Yeh et al. 1996).

Particle deposition experiments have been performed using human volunteers or laboratory animals (Landahl 1950; Lippmann et al. 1971; Giacomelli-Maltoni et al. 1972; Heyder et al. 1975; Schlesinger and Lippmann 1976; Raabe et al. 1988), hollow casts of surgically-removed lungs (Schlesinger and Lippmann 1972, 1976; Schlesinger et al. 1977; Cohen et al. 1990), and idealized respiratory tract models (Bell and Friedlander 1973; Schlesinger and Lippmann 1976; Ferron 1977; Martonen 1983; Phalen et al. 1989). For the most part, these studies have addressed particle deposition in the adult respiratory tract, without provisions for scaling airflows and airway dimensions to values relevant to children. However, a few studies dealing with the age-dependency of particle deposition in the respiratory tract have been performed. Hofmann (1982) developed a theoretical age-dependent lung morphology and examined effects on particle deposition of scaling airway anatomical parameters and airflow rates; they concluded that particle deposition is strongly dependent upon age, with children having significantly higher doses than adults. Xu and Yu (1986) also examined particle deposition as a function of age. In modeling aerosol deposition in the respiratory tract, they found higher total deposition in children than adults; but for tracheobronchial and alveolar deposition, the age dependence was a function of particle size. These models used theoretical anatomical geometries. More accurate anatomical data obtained from measurements of lung casts of 21 children and adolescents, along with body size-scaled airflows and the mathematical approach of Yeh and Schum

* Air Pollution Health Effects Laboratory, Department of Community and Environmental Medicine, FRF, Room 8, University of California, Irvine, CA 92697-1825.

(*Manuscript received* 1 *July* 1996; *revised manuscript received* 10 *October* 1996, *accepted* 9 *January* 1997)

0017-9078/97/$3.00/0

Table 1. Geometrical parameters of tracheobronchial models[a].

	Four-y-old[c]		Seven-y-old		Adult	
Generation[b]	Diameter (mm)	Length (mm)	Diameter (mm)	Length (mm)	Diameter (mm)	Length (mm)
1	10.8	54.6	13.1	68.9	18.2	89.0
2	8.1	25.5	9.7	29.6	13.0	38.3
3	5.7	9.7	6.9	11.3	9.0	14.7
4	N/A	N/A	5.1	8.0	6.7	10.5

[a] All branch angles = 45°; the trachea was vertical in all cases, and the average inclination to gravity for generations 2–4 was 45°.
[b] Trachea = 1.
[c] The four-y-old model was limited to three generations due to the fabrication technique.

(1980), were used to obtain estimates of tracheobronchial deposition efficiency for infants, children and adolescents (Phalen et al. 1988). In general, it was determined that children may exhibit a higher tracheobronchial deposition efficiency than adults for most particle sizes (between 0.01 and 100 μm) and states of activity (i.e., ventilation rates). In a study employing idealized hollow nasal models, it was concluded that the nasal cavities of children and adults have similar deposition efficiencies, but that the higher body-mass-specific ventilation rate of children leads to a greater deposition of particles in children in relation to the body mass of the exposed individual (Phalen et al. 1989). Swift (1991) used *in-vivo* magnetic resonance images to construct replica nasal casts of an adult and infant. Using particles from 1 to 10 μm, he also found that at equivalent states of activity, deposition efficiencies for the adult and infant were similar. Martonen et al. (1989) used two different body-size-scaled morphologies and concluded that total respiratory tract deposition is greater for children than for adults. Both the ICRP and proposed NCRP dosimetry models include theoretical adjustments for calculating aerosol deposition in children.

The present study was performed to determine if these predictions of greater deposition in children could be validated for the upper tracheobronchial airways using scaled idealized hollow tracheobronchial models. Such effects, if they exist, could have a bearing on the assessment of the risks attendant to inhalation of aerosols associated with nuclear power-generation, medical treatments, and natural radioactive particulate material (attached radon progeny, etc.) in ambient air.

MATERIALS AND METHODS

Hollow tracheobronchial models

Coplanar single-pathway hollow models representing the large tracheobronchial airways were fabricated using a lost-wax technique (Oldham 1977; Martonen 1983). The model representing the airways of an adult (18 y-old) was designed using geometric parameters from measurements of 21 lung casts (Phalen et al. 1985). Two smaller models were constructed so that the average airway dimensions (lengths and diameters) were 77% and 65% of those of the adult model. The geometric parameters of all three sizes of tracheobronchial models are shown in Table 1. The tracheal diameters of the 77%-size and 65%-size models are within about 7% of the tracheal diameters predicted for a 7-y-old child and 4-y-old child, respectively (Phalen et al. 1985). The branch angles for all non-tracheal generations were set at 45° (equivalent to bifurcation angles of 90°) so that all generations after the trachea had average inclination to gravity angles of 45°, and for ease of construction. The models were not preceded by a larynx because laryngeal jet dimensions during inhalation are uncertain for children; although Mostafa (1976) reported results of measurements of endotracheal tube diameters (presumed to be the maximum diameter that would fit through the larynx), his study was performed under anesthesia and utilized a muscle relaxant, so it is uncertain how these measurements in children aged 3 mo to 13 y relate to normal laryngeal jet dimensions during inhalation. However, it is recognized that the laryngeal jet can have a substantial influence on particle deposition in the trachea and major bronchi (Gurman et al. 1980).

Hollow models (Fig. 1) were fabricated using room-temperature vulcanizing silicone rubber—either Silastic® E[†] or RTV 664.[‡] These materials were selected for their negligible shrinkage on curing and their cured strength. The models were fitted with smooth transition connectors to the particle generation system and to the exit filters from the models (Fig. 2). Model airway segments, which were connected to exit filters, were designed to have airway lengths of 150% of the lengths specified in Table 1 in order to reduce the influence of downstream turbulence, which could affect the upstream deposition of particles. However, only deposition in the appropriate lengths of the airways was included in the data analysis as representing particles which deposited in the model (the remainder was included with the filter deposition). Particle deposition experiments were conducted at steady (uni-directional) inspiratory airflows which represented a state of low physical activity for each age represented by a hollow model: 20 L min^{-1} for the adult; 9 L min^{-1} for the 7-y-old child; and 5.5 L min^{-1} for the 4-y-old child (Phalen et al. 1985). During the particle depositions, the models were mounted on supports to maintain desired branch angles and airway

[†] Silastic® E, Dow Corning, Midland, MI 48686-0994.
[‡] RTV 664, General Electric Co., Waterford, NY 12186.

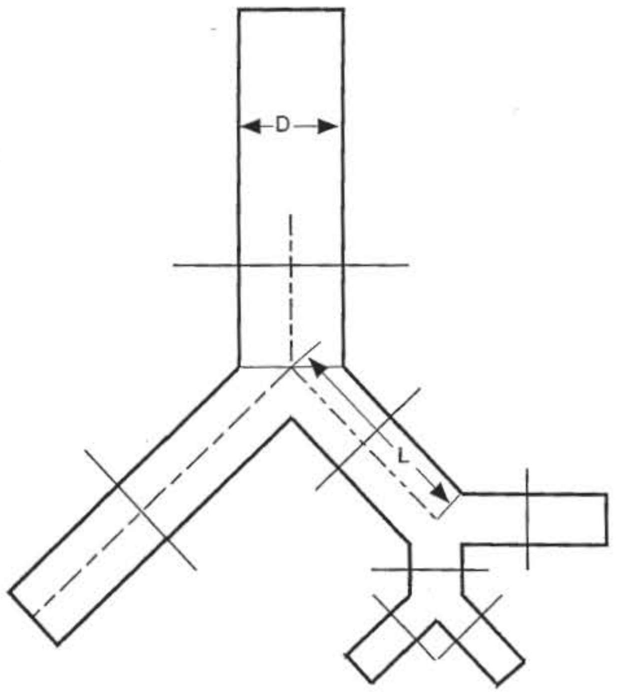

Fig. 1. Representation of the three generation adult hollow tracheobronchial model (approximately to scale). With reference to values in Table 1, the airway diameter D and length L are shown. Cut lines for dividing the model into segments for radiation counting are also shown.

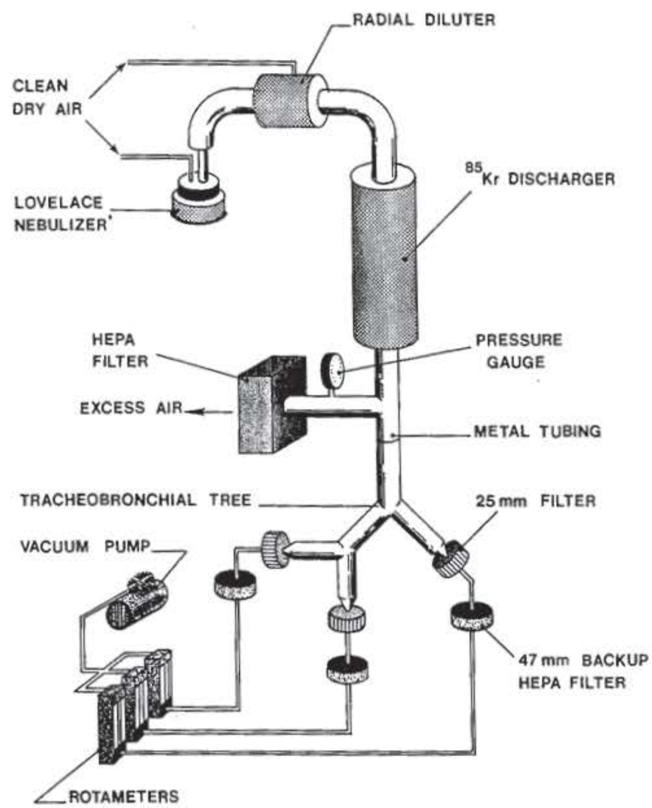

Fig. 2. The particle generation and sampling system, and two generation 4-y-old hollow tracheobronchial model (not to scale). The hollow models were oriented in a vertical position, as shown.

inclinations to gravity (trachea vertical, etc.). For each experimental condition, duplicate runs were conducted to ensure reproducibility.

Particle generation and deposition

Four sizes of monodisperse radiolabeled microspheres were used in the study: 1.2 μm, 4.5 μm, 9.7 μm, and 15.4 μm (nominal diameters). The three largest sizes of particles were polystyrene particles (density = 1.23 g cm^{-3}) obtained from a commercial supplier.[§] The 1.2 μm particles were polystyrene latex (density = 1.05 g cm^{-3}) and were produced in our laboratory in accordance with the method of Hinrichs et al. (1978). The 1.2 μm and 4.5 μm values are activity median aerodynamic diameters (AMADs), which were determined by sizing the particles with a seven-stage Mercer-type impactor[‖] with a back-up glass fiber filter. The AMAD (assuming that the quantity of radiolabel is directly proportional to the particle mass) of the two largest sizes of particles were calculated using data provided by the supplier (verified at our laboratory using light microscopy) and the Hatch-Choate equations (Hatch and Choate 1929). The geometrical standard deviations (GSDs) were about 1.1–1.2. Each size of particle was radiolabeled with a different radionuclide: 1.2 μm particles with ^{51}Cr; 4.5 μm particles with ^{54}Mn; 9.7 μm particles with ^{141}Ce; and 15.4 μm particles with ^{85}Sr. Due to the excellent resolution of the radiation detector, two sizes of particles could be deposited, with deposits separately analyzed in the same experiment. The two large particle sizes (9.7μm and 15.4μm) were used since replicate infant and adult nasal cast experiments by Swift (1991) indicated that approximately 5% of particles as large as 15.4 μm particles could penetrate beyond the nose and be available for deposition in the larynx and upper tracheobronchial airways.

A Lovelace-type compressed air nebulizer[‖] was used to generate the radioactive aerosols. The nebulizer was modified by enlarging the air jet in the nebulizer stem from the original diameter of 0.23 mm up to a diameter of about 0.4 mm, and by removing the baffle, thus enabling the 9.7 μm and 15.4 μm particles to be generated in quantities sufficient for the deposition experiments. Aerosols were generated at a nebulizer pressure of 1.4 kg cm^{-2} (20 psi) from 0.1–0.3% (by volume) aqueous suspensions of the particles in distilled water. All particle suspensions were sufficiently dilute to preclude the generation of more than 10% of the particles as muliplets (Raabe 1968). The aerosols were dried and diluted using a radial diluter that injected dry (5% RH) air into the airstream (Fig. 2). The quantity of air used for

[§] 3M, St. Paul, MN 55144-1000; Note: 3M no longer supplies radiolabeled microspheres.

[‖] Model 02-140 Mercer-type impactor and Lovelace type nebulizer as described in Raabe (1972). In-Tox Products, Albuquerque, NM 87108.

dilution was 10 times that put out by the nebulizer. After passing through a 0.37 GBq ^{85}Kr discharger, particle-laden air was pulled by a vacuum pump through the hollow model. Particles that did not deposit in the model were captured on 25-mm diameter glass fiber exit filters. The airflow through each exit of the hollow model was controlled by a rotameter calibrated using a spirometer. The entire airflow (5.5, 9, or 20 L min^{-1}) traversed the tracheal section. Just beyond the first bifurcation, each of the two simulated airways carried one-half of the total airflow. Just beyond the second bifurcation, each of the two airways carried one-quarter of the total airflow, and so on. Since the airflow exiting the discharger exceeded the hollow tracheobronchial model flow rate, it was necessary to discard excess particle-laden air passively through a HEPA (high-efficiency particulate air) filter.

The experimental setup used for the deposition experiments was housed in a 1 m^3 volume secondary containment chamber, which was maintained at a pressure slightly negative with respect to the room. The exhaust from this chamber was passed through a HEPA filter. Prior to each experiment, the hollow model setup was leak-tested by pressurizing it to at least 5 cm of water column. A pressure loss of less than 0.25 cm of water over 20 s was required before a setup was used in an experiment. The duration of the particle deposition phase of the experiments was based on the amount of time necessary to deposit sufficient quantities of particles to provide for acceptable radiation counting statistics.

Sample preparation and radiation counting

After the deposition of radiolabeled particles, the models were cut into segments which were then placed into plastic petri dishes. In order to maximize the radiation counting sensitivity and to allow for a relatively-consistent counting geometry, the model segments were flattened (compressed) with folded paper towels on top in the petri dishes. In this way, the solid angle presented by each segment to the radiation detector was similar when counting the various segments, which varied in size. Exit filters and filter cassettes were placed into small plastic bags prior to counting to prevent contamination of the radiation detector. Although the filter cassettes were not compressible, and necessarily presented a somewhat different counting geometry to the detector, they generally had negligible quantities of deposited radioactivity, as compared with the radioactivity deposited on the filters. All radioactive samples were counted by centering them directly on top of a lead-shielded 7.6 cm × 7.6 cm NaI(Tl) gamma ray detector interfaced with amplifiers and a multichannel analyzer.[¶] The resolution of the counting apparatus easily permitted separation of the gamma ray photopeaks in the cases in which two sizes of particles (labeled with different radionuclides) were deposited in the same experiment. Since some counts were present in the lower gamma ray energy photopeak due to the presence of the higher gamma ray energy nuclide in the counting samples, the fraction of the net counts in the higher-energy photopeak that appeared in the lower-energy nuclide counting region was subtracted. All samples were counted for sufficient periods of time to ensure that statistical uncertainty due to counting errors was less than 5%. Calculations were performed to normalize the radioactivity in the model segments to the total, including that which passed through the segment without depositing in it. Radioactivity that deposited in the additional airway exit lengths or beyond was considered to be radioactivity which did not deposit in the hollow model.

Investigation of particle bounce and re-entrainment effects

A set of experiments was initially performed to determine whether or not particle bounce and/or particle re-entrainment would introduce artifacts. These experiments were undertaken in order to determine the necessity of coating the interior of the models prior to performing deposition experiments. The experiments involved the adult-size hollow model, an airflow of 20 L min^{-1} (the highest airflow used in any of the deposition experiments), and the ^{85}Sr-labeled 15.4 μm particles (the largest particles used). In the first experiment, the model was coated with a thin layer of petroleum jelly, which had been liquefied by heating and then poured through the model until all of the airways were coated with a very thin layer. The 15.4 μm particles were then deposited in the model using the same protocol employed in the other experiments.

The model was cut up as described above, and the model segments, extra airway lengths, exit filters and filter cassettes were analyzed for ^{85}Sr radioactivity. The same methodology was employed in the second experiment; however, in this case the hollow model was not coated with petroleum jelly. The results of the two experiments were similar with respect to the total deposition percentage measured and the deposition pattern of the particles within the models. Therefore, particle bounce was excluded as a significant source of experimental error. In another (re-entrainment) experiment, the 15.4 μm particles were initially deposited in an uncoated model at 20 L min^{-1}. The exit filters and filter cassettes were removed and analyzed for ^{85}Sr radioactivity. These items were replaced with new, unused filters and cassettes, and filtered dilution air was pulled through the model at 20 L min^{-1} for 10 min. The model was subsequently cut up, and the model segments, extra airway lengths, filters and filter cassettes were analyzed for ^{85}Sr radioactivity. Since the regional deposition pattern was similar to that observed in the case of the coated model, and because only a negligible quantity of radioactivity was measured on the second sets of filters and cassettes, it was concluded that particle re-entrainment was also not a significant source of error in the deposition experiments.

¶ Model TN-7200 Multichannel Analyzer, Tracor Northern, Middleton, WI 53562.

RESULTS

As the 4-y-old hollow model consisted of three generations (trachea = generation 1), only the first three generations of the 7-y-old and adult were included in intercast comparisons. The results of the particle deposition experiments are shown in Table 2. As would be expected for particles in this size range, for each of the three sizes of tracheobronchial model, the greater the particle diameter, the greater the deposition efficiency. An ANOVA demonstrated statistically-significant main effects of particle size and size of hollow model; the interaction between the two was likewise significant at a p value of 0.05. Therefore, the deposition efficiency is a function of the size of model, which is related to the age of the exposed individual.

Fig. 3a, b and c are plots of the percent particle deposition vs. particle diameter for the 4-y-old, 7-y-old and the adult, respectively. The results of each of the two trials for each experimental condition are shown. The average detection level for the data, which is related to the radiation counting statistics, is also given.

DISCUSSION

This study was performed to determine the effects of particle size and hollow tracheobronchial model size (as an analog for age of individual), and the interaction of these two variables, on deposition efficiency of monodisperse particles in hollow models representing adult and child-size tracheobronchial airways. The results demonstrated statistically-significant effects of particle size and model size, and their interaction. From an examination of the particle deposition results shown in Table 2, it is apparent that (a) the larger the particle size, the greater the deposition efficiency, and (b) deposition efficiencies were greater for the child-size models than for the adult-size in nearly all cases studied. The increase in deposition efficiency with particle size was expected, and has been described by Schlesinger and Lippmann (1976) and Martonen (1983), among others. The finding that the deposition efficiency was more pronounced for child-size models agrees with the theoretical predictions (Hofmann 1982; Xu and Yu 1986; Phalen et al. 1988; Martonen et al. 1989). Our results in Table 2 also show that for particles ≥ 4.5 μm, deposition in the 7-y-old was higher than deposition in the 4-y-old and adult. The theoretical predictions of Xu and Yu (1986) have a similar pattern only for total deposition (tracheobronchial and pulmonary) for mouth breathing; however, the maximum deposition occurred in the 2-y-old in their study. It is not clear if our result is real or an anomaly, due in some part to any differences in airway smoothness between the three sizes of hollow tracheobronchial models, a result of a combination of airway size scaling and scaled ventilation or possible electrostatic charge phenomena. The significance of the effect of electrostatic charge on deposition of 2–7 μm particles in hollow silicone rubber larynx-tracheobronchial casts has been shown (by Chan et al. 1978) to be consistent with theoretical predictions (Yu 1977). Even though the aerosol was discharged to Boltzmann equilibrium, most individual particles still carry some charge. Since the Silastic hollow tracheobronchial models were non-conducting, it is possible that charge islands existed and preferential deposition occurred. Although no obvious charge islands were observed when the casts were cut into pieces for counting, it is possible that some of the variability seen in results shown in Table 2 could be due to electrostatic effects.

The mathematical formulation of Yeh and Schum (1980) was used to compare the experimentally-determined results with the results obtained using theoretical deposition predictions. Their equations, which are used in the proposed NCRP lung dosimetry model, predict deposition based upon the mechanisms of impaction, sedimentation, and diffusion, together with airway geometry and airflow information. Airway length, diameter, and branch angle dimensions from the hollow models were used as anatomical input into the equations.

Table 2. Measured tracheobronchial deposition efficiencies (%). Significant ($p < 0.05$) main effects of particle size ($F = 61.4$) and model size ($F = 5.3$); significant interaction between variables ($F = 3.5$).

Model	Deposition efficiency (%)[a] Particle diameter[b] 1.2	4.5	9.7	15.4
Four-y-old Total	0.3 ± 0.04	0.27 ± 0.05	1.69 ± 0.25	10.7 ± 4.3
Trachea	0.19 ± 0.08	0.01 ± 0.01	0.12 ± 0.03	0.46 ± 0.19
Bifurcation 1	0.11 ± 0.005	0.06 ± 0.05	1.00 ± 0.24	7.54 ± 2.99
Bifurcation 2	0.0	0.2 ± 0.005	0.56 ± 0.01	2.7 ± 1.08
Seven-y-old Total	0.04 ± 0.03	0.36 ± 0.13	2.66 ± 0.6	17.6 ± 0.6
Trachea	0.0	0.12 ± 0.03	0.41 ± 0.3	4.26 ± 1.57
Bifurcation 1	0.04 ± 0.03	0.15 ± 0.04	1.52 ± 0.22	9.72 ± 1.68
Bifurcation 2	0.0	0.09 ± 0.06	0.72 ± 0.08	3.59 ± 0.62
Adult Total	0.05 ± 0.01	0.04 ± 0.03	1.26 ± 0.03	7.9 ± 0.3
Trachea	0.03 ± 0.03	0.0	0.36 ± 0.03	1.13 ± 0.16
Bifurcation 1	0.02 ± 0.02	0.02 ± 0.02	0.53 ± 0.06	4.15 ± 0.38
Bifurcation 2	0.0	0.02 ± 0.01	0.38 ± 0.05	2.62 ± 0.52

[a] Deposition efficiency expressed as a percentage; mean ± range, with $N = 2$.
[b] Particle AMAD in μm.

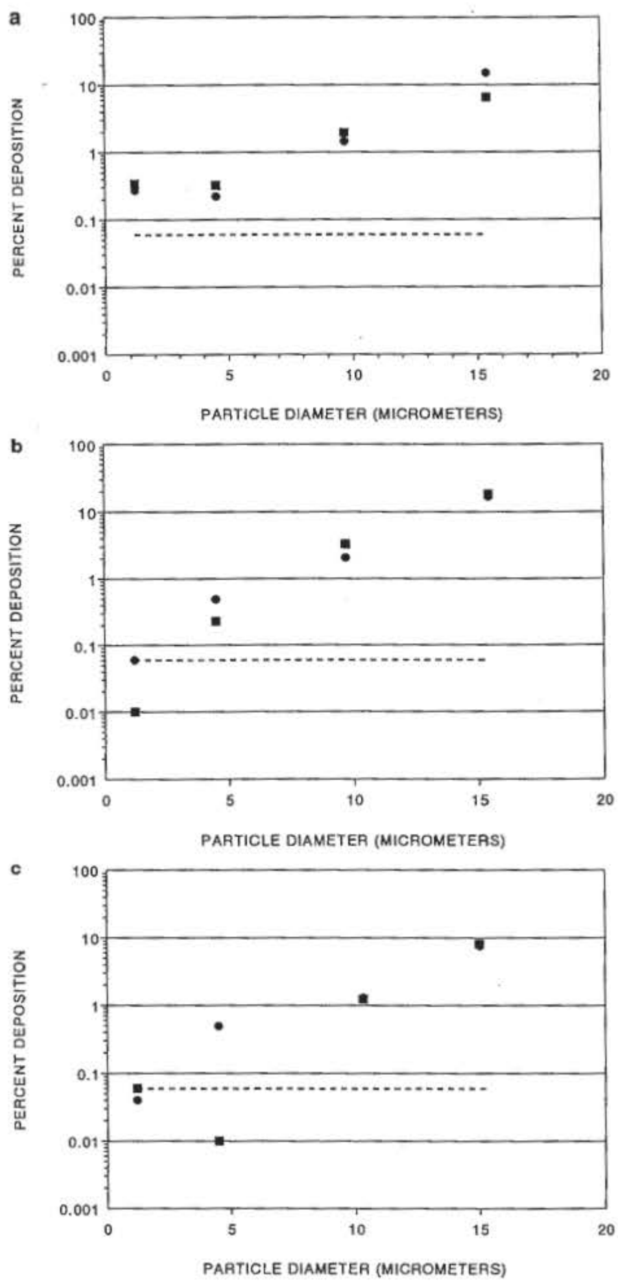

Fig. 3. Experimentally-observed particle deposition percentage vs. particle diameter data: (a) 4-y-old child model; (b) 7-y-old child model; (c) adult model. The first run (■), second run (●), and average detection limit (- - - -) are shown.

Measured flow rates and AMADs were also used in the predictions. The equations provide deposition on a generation-by-generation basis, which enables bifurcation units to be constructed from the program output to match those of the hollow models. The results (Fig. 4) indicate that the best agreement between predicted and experimental results occurs for the largest size particles (15.4 μm). In all other cases, the mathematical formulation predicted higher deposition efficiency than was

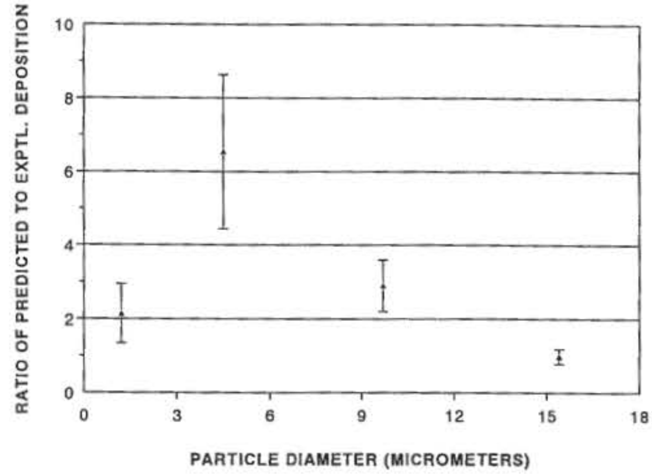

Fig. 4. Ratio of computer-model-predicted deposition results to those obtained experimentally for all three hollow tracheobronchial models (values below detection limits were excluded); means ± SE are displayed.

measured. One possible explanation is that the mathematical models assumed either fully developed turbulent or laminar flow, neither of which existed in the hollow tracheobronchial models. Cohen et al. (1993) measured skewed velocity profiles and unsteady flows in replica human casts at constant inspiratory flow rates as low as 7.5 L min^{-1}. Dekker (1961) observed non-laminar tracheal flow for constant inspiratory flows as low as 3.1 L min^{-1}.

Usually the airway Reynolds number (*Re*), which is a ratio of viscous to inertial forces, is used as a measure of laminar or turbulent airflow. *Re* is defined as

$$Re = \rho V d \eta^{-1}, \tag{1}$$

where ρ is the density of air, V is the air velocity, d is the tube diameter and η is the viscosity of air. In smooth walled tubes, $Re < 2{,}000$ indicating a laminar flow regime, with $Re > 10{,}000$ indicating fully developed turbulent flow. The *Re* regime between 2,000 and 10,000 represents a transition region. Fig. 5 shows the *Re* for each generation of hollow tracheobronchial models used in our study. It should be noted that the hollow tracheobronchial models are relatively smooth, short bifurcating tubes, and that fully-developed laminar flow may only exist at significantly lower *Re* values. Based upon the observation of Clarke et al. (1972) that secondary flows (flows in directions other than the airway centerline) occurred in bifurcating tubes with a *Re* of 100, it is likely that secondary flows existed in our hollow tracheobronchial models. These secondary flows are likely to depend on the *Re* and the bifurcating nature of the models. Olson et al. (1970) defined an entrance length (*Le*) required to fully develop laminar flow:

$$Le = 0.02875\ D\ Re. \tag{2}$$

The *Le* is based on airway diameter (D) and Reynolds number (*Re*). Table 3 shows the entrance length required

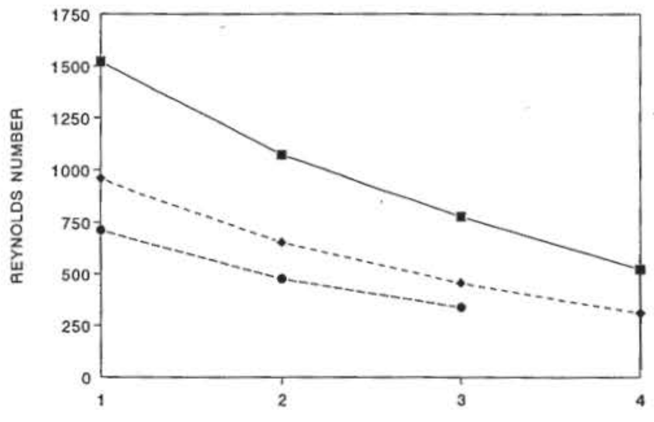

Fig. 5. Reynolds number vs. airway generation (trachea = generation 1) for each size of hollow tracheobronchial model: 4-y-old (●), 7-y-old (♦), and adult (■).

Table 3. Entrance length (Le) required for fully-developed laminar flow in hollow tracheobronchial models.

	Le (mm)		
Generation[a]	Four-y-old	Seven-y-old	Adult
1	221	362	796
2	111	182	401
3	55	90	201
4	N/A	45	101

[a] Trachea = 1.

to fully develop laminar flow in our hollow tracheobronchial models. A comparison with the airway lengths from Table 2 indicates that our airway lengths were between 2.3% and 11.3% of the necessary lengths required for fully developed laminar flow. It appears that the flow profiles in hollow tracheobronchial models are extremely complex and are probably not adequately dealt with in the mathematical formulations used for the comparison.

If impaction were the only mechanism influencing deposition, the Stokes number (Stk.) would be tightly correlated with deposition efficiency. Plots of deposition vs. Stk. show an upward trend, but considerable scatter is seen. This scatter is due to effects including particle sedimentation and experimental variations (along with any electrostatic effects). It is clear that the Stk. number is important, but it is not predictive of any given result.

CONCLUSIONS

The finding that deposition efficiency is more pronounced for child-size models indicates that children could be more susceptible to upper bronchial effects from exposure to aerosol particles with aerodynamic diameters above 1 μm. Common non-radioactive particulate in this size range includes allergens such as mold spores, pollens and excreta from dust mites and cockroaches, and some of the major components in outdoor PM_{10}, such as road dust and other mechanically-generated particulate materials. Radioactive particulate in this size range includes surface dusts, particulate-attached radon progeny, and soil at nuclear weapons test sites (Stradling et al. 1992). Our measurements are consistent with the predictions of the proposed NCRP model, but as our deposition efficiencies were lower, the radiation protection model may be conservative in that it overestimates the upper tracheobronchial deposition. Since children also have higher body-mass-specific ventilation rates (i.e., per kg of body mass) than adults, and seem to be more susceptible to inflammatory respiratory responses such as asthma, allergies, and bronchitis than are healthy non-senescent adults, it may be appropriate to include airway-size factors in risk assessments related to airborne particulate in the ambient air.

Acknowledgments—The authors thank G. Michael Schum, William Mautz and Michael Kleinman for their technical assistance, and Marie Tonini for word processing the manuscript. The research was supported by the National Heart, Lung and Blood Institute (RO1 HL39682). Dr. Phalen is supported by the University of California, Irvine Center for Occupational and Environmental Health.

REFERENCES

Balásházy, I.; Hofmann, W.; Martonen, T. B. Inspiratory particle deposition in airway bifurcation models. J. Aerosol Sci. 22:15–30; 1991.

Bell, K. A.; Friedlander, S. K. Aerosol deposition in models of a human lung bifurcation. Staub-Reinhalt. Luft 33:178–182; 1973.

Chan, T. I.; Lippmann, M.; Cohen, V. R.; Schlesinger, R. B. Effect of electrostatic charges on particle deposition in a hollow cast of the human larynx-tracheobronchial tree. J. Aerosol Sci. 9:463–468; 1978.

Clarke, S. W.; Jones, J. G.; Oliver, D. R. Factors affecting airflow through branched tubes. Bull. Physiopathol. Respir. 8:408–428; 1972.

Cohen, B. S.; Sussman, R. G.; Lippmann, M. Ultrafine particle deposition in a human tracheobronchial cast. Aerosol Sci. Technol. 12:1082–1091; 1990.

Cohen, B. S.; Sussman, R. G.; Lippmann, M. Factors affecting distribution of airflow in a human tracheobronchial cast. Res. Physiol. 93:261–278; 1993.

Dekker, E. Transition between laminar and turbulent flow in human trachea. J. Appl. Physiol. 16:1060–1064; 1961.

Ferron, G. A. Deposition of polydisperse aerosols in two glass models representing the upper human airways. J. Aerosol Sci. 8:409–427; 1977.

Giacomelli-Maltoni, G.; Melandri, C.; Prodi, V.; Tarroni, G. Deposition efficiency of monodisperse particles in human respiratory tract. Am. Ind. Hyg. Assoc. J. 33:603–610; 1972.

Gurman, J. L.; Schlesinger, R. B.; Lippmann, M. A variable-opening mechanical larynx for use in aerosol deposition studies. Am. Ind. Hyg. Assoc. J. 41:678–680: 1980.

Hatch, T.; Choate, S. Statistical description of the size properties of non-uniform particle substances. J. Franklin Inst. 207:369–387; 1929.

Heyder, J.; Armbruster, L.; Gebhart, J.; Grein, E.; Stahlhofen, W. Total deposition of aerosol particles in the human respiratory tract for nose and mouth breathing. J. Aerosol Sci. 6:311–328; 1975.

Hinrichs, R. J.; Kenoyer, J. L.; Phalen, R. F; Crocker, T. T. Labeling of monodisperse polystyrene microspheres with tightly-bound ^{51}Cr. Am. Ind. Hyg. Assoc. J. 39:570–575; 1978.

Hofmann, W. Dose calculations for the respiratory tract from inhaled natural radioactive nuclides as a function of age—II. Health Phys. 43:31–44; 1982.

Landahl, H. On the removal of airborne droplets by the human respiratory tract. I. The lung. Bull. Math. Biophys. 12:43–56; 1950.

Lippmann, M.; Albert, R. E.; Petersen, H. T., Jr. The regional deposition of inhaled aerosols in man. In: Walton, W. H., ed. Inhaled Particles III, Vol. 1. Old Working Surrey, United Kingdom: Unwin Brothers Limited; 1971:105–122.

Martonen, T. B. Measurement of particle dose distribution in a model of a human larynx and tracheobronchial tree. J. Aerosol Sci. 14:11–22; 1983.

Martonen, T. B.; Graham, R. C.; Hofmann, W. Human subject age and activity level: Factors addressed in a biomathematical deposition program for extrapolation modeling. Health. Phys. 57(Suppl.):49–59; 1989.

Morrow, P. E.; Bates, D. V.; Fish, B. R.; Hatch, T. F.; Mercer, T. T. Deposition and retention models for internal dosimetry of the human respiratory tract. Health Phys. 12:173–207; 1966.

Oldham, M. J. Hollow tracheobronchial casts for use in aerosol deposition studies. Univ. of California, Irvine. J. Undergrad. Res. 7:456–465; 1977.

Olson, D. E.; Dart, G. A.; Filley, G. F. Pressure drop and fluid flow regime of air inspired into the human lung. J. Appl. Physiol. 28:482–494; 1970.

Mastafa, S. M. Variation in subglottic size in children. Proc. Roy. Soc. Med. 69:793–795;1976.

Phalen, R. F.; Oldham, M. J.; Beaucage, C. B.; Crocker, T. T.; Mortensen, J. D. Postnatal enlargement of human tracheobronchial airways and implications for particle deposition. Anat. Rec. 212:368–380; 1985.

Phalen, R. F.; Oldham, M. J.; Kleinman, M. T.; Crocker, T. T. Tracheobronchial deposition predictions for infants, children and adolescents. Ann. Occup. Hyg. 32(Suppl.):11–21; 1988.

Phalen, R. F.; Oldham, M. J.; Mautz, W. J. Aerosol deposition in the nose as a function of body size. Health Phys. 57(Suppl.):299–305; 1989.

Raabe, O. G. The dilution of monodisperse suspensions for aerosolization. Am. Ind. Hyg. Assoc. J. 29:439–443; 1968.

Raabe, O. G. Operating characteristics of two compressed air nebulizers used in inhalation experiments. In: Fission Product Inhalation Program Annual Report 1971–1972. Inhalation Toxicology Research Institute, Albuquerque, N.M. LF-45:1–6; 1972.

Raabe, O. G.; Al-Bayati, M. A.; Teague, S. V.; Rasolt A. Regional deposition of inhaled monodisperse coarse and fine aerosol particles in small laboratory animals. Ann. Occup. Hyg. 32(Suppl.):53–63; 1988.

Schlesinger, R. B.; Lippmann, M. Particle deposition in casts of the human upper tracheobronchial tree. Am. Ind. Hyg. Assoc. J. 33:237–251; 1972.

Schlesinger, R. B.; Lippmann, M. Particle deposition in the trachea: in vivo and in hollow casts. Thorax 31:678–684; 1976.

Schlesinger, R. B.; Bohning, D. E.; Chan, T. L.; Lippmann, M. Particle deposition in a hollow cast of the human tracheobronchial tree. J. Aerosol Sci. 8:429–445; 1977.

Schum, G. M.; Phalen, R. F.; Oldham, M. J. Risk assessment of inhaled particles: Integrating time-activity patterns with respiratory tract particle deposition models. Ann. Occup. Hyg. 38(Suppl.):973–978; 1994.

Stradling, G. N.; Stather, J. W.; Gray, S. A.; Moody, J. C.; Ellender, M.; Pearce, M. J.; Collier, C. G. Radiological implications of inhaled ^{239}Pu and ^{241}Am in dusts at the former nuclear test site in Maralinga. Health Phys. 63:641–650; 1992.

Swift D. L. Age-related scaling for aerosol and vapor deposition in the upper airways of humans. Health Phys. 57(Suppl.):293–297; 1989.

Swift, D. L. Inspiratory inertial deposition of aerosols in human nasal airway replicate casts: implication for the proposed NCRP lung model. Radiat. Prot. Dosim. 38:29–34; 1991.

Thomas, R. G. Regional human lung dose following inhalation of radioactive particles at ages one month to adulthood. Ann. Occup. Hyg. 32(Suppl.):1025–1033; 1988.

Xu, G. B.; Yu, C. P. Effects of age on deposition of inhaled aerosols in the human lung. Aerosol Sci. Technol. 5:349–357; 1986.

Yeh, H. C.; Phalen, R. F.; Raabe, O. G. Factors influencing the deposition of inhaled particles. Environ. Health Perspect. 15:147–156; 1976.

Yeh, H. C.; Schum, G. M. Models of human lung airways and their application to inhaled particle deposition. Bull. Math. Biol. 42:461–480; 1980.

Yeh, H. C.; Cuddihy, R. G.; Phalen, R. F.; Chang, I. Y. Comparisons of calculated respiratory tract deposition of particles based on the proposed NCRP model and the new ICRP66 model. Aerosol Sci. Technol. 25:134–140; 1996.

Yu, C. P. Precipitation of charged particles in cylindrical and spherical vessels. J. Aerosol Sci. 8:237–241; 1977.

■ ■